The filamentary structure of mixing fronts and its control on reaction kinetics in porous media flows

Pietro de Anna, Marco Dentz, Alexandre Tartakovsky, Tanguy Le Borgne

▶ To cite this version:

Pietro de Anna, Marco Dentz, Alexandre Tartakovsky, Tanguy Le Borgne. The filamentary structure of mixing fronts and its control on reaction kinetics in porous media flows. Geophysical Research Letters, 2014, 41 (13), pp.4586-4593. 10.1002/2014GL060068 . insu-01053589

HAL Id: insu-01053589

https://insu.hal.science/insu-01053589

Submitted on 31 Jul 2014

HAL is a multi-disciplinary open access archive for the deposit and dissemination of scientific research documents, whether they are published or not. The documents may come from teaching and research institutions in France or abroad, or from public or private research centers.

L'archive ouverte pluridisciplinaire HAL, est destinée au dépôt et à la diffusion de documents scientifiques de niveau recherche, publiés ou non, émanant des établissements d'enseignement et de recherche français ou étrangers, des laboratoires publics ou privés.

AGU PUBLICATIONS

Geophysical Research Letters

RESEARCH LETTER

10.1002/2014GL060068

Key Points:
- We propose a new model based on stretching, coalescence, and dispersion
- The coalescence of filament-like structures impact the global reaction kinetics
- Our model provides a framework for predicting heterogeneous front kinetics

Correspondence to:
P. de Anna,
pietrodeanna@gmail.com

Citation:
de Anna, P., M. Dentz, A. Tartakovsky, and T. Le Borgne (2014), The filamentary structure of mixing fronts and its control on reaction kinetics in porous media flows, *Geophys. Res. Lett.*, *41*, doi:10.1002/2014GL060068.

Received 18 APR 2014
Accepted 28 MAY 2014
Accepted article online 1 JUN 2014

The filamentary structure of mixing fronts and its control on reaction kinetics in porous media flows

Pietro de Anna[1], Marco Dentz[2], Alexandre Tartakovsky[3,4], and Tanguy Le Borgne[5]

[1] Department of Civil and Environmental Engineering, Massachusetts Institute of Technology, Cambridge, Massachusetts, USA, [2] Spanish National Research Council, IDAEA-CSIC, Barcelona, Spain, [3] School of Geosciences, Department of Mathematics and Statistics, University of South Florida, Tampa, Florida, USA, [4] Pacific Northwest National Laboratory, Richland, Washington, USA, [5] UMR 6118, CNRS, Université de Rennes 1, Rennes, France

Abstract The mixing dynamics resulting from the combined action of diffusion, dispersion, and advective stretching of a reaction front in heterogeneous flows leads to reaction kinetics that can differ by orders of magnitude from those measured in well-mixed batch reactors. The reactive fluid invading a porous medium develops a filamentary or lamellar front structure. Fluid deformation leads to an increase of the front length by stretching and consequently a decrease of its width by compression. This advective front deformation, which sharpens concentration gradients across the interface, is in competition with diffusion, which tends to increase the interface width and thus smooth concentration gradients. The lamella scale dynamics eventually develop into a collective behavior through diffusive coalescence, which leads to a disperse interface whose width is controlled by advective dispersion. We derive a new approach that quantifies the impact of these filament scale processes on the global mixing and reaction kinetics. The proposed reactive filament model, based on the elementary processes of stretching, coalescence, and fluid particle dispersion, provides a new framework for predicting reaction front kinetics in heterogeneous flows.

1. Introduction

Reactive fronts and mixing interfaces play a central role in controlling the chemical and biological evolution of many natural and industrial systems [*Renard et al.*, 1998; *De Wit*, 2001]. In particular, mixing and reaction processes occurring in flow through porous media have recently received increasing attention because they play a key role in a number of important applications, including CO_2 storage and oil recovery in geological formations [*Szulczewski et al.*, 2012; *Ennis-King and Paterson*, 2005], fracture pattern formation [*Malthe–Sorenssen et al.*, 2006], reaction-enhanced permeability [*Jamtveit et al.*, 2008], nutrient transport [*Durham et al.*, 2011], large-scale water contamination of anthropogenic or geogenic elements such as nitrate [*Sebilo et al.*, 2013] and arsenic [*Polizzotto et al.*, 2005], and the temporal evolution of water quality in rivers over a range of scales [*Kirchner and Neal*, 2013]. For all these mixing-dependent systems, the large-scale behavior depends upon the microscale distribution of chemical and physical gradients. Classical Fickian transport theories, which assume that chemical species are well mixed at the relevant support scale, are known to be inaccurate for these systems [*Tartakovsky et al.*, 2009; *Dentz et al.*, 2011]. Fluid flow in porous media has been shown to be characterized by a strong intermittency [*de Anna et al.*, 2013], which implies that mesoscale mass fluxes do not follow Fick's law. However, the impact of the resulting incomplete mixing processes and non-Fickian dispersion on the global reaction kinetics is still an open issue.

Reaction rates in fluid flows are determined by the interaction of microscopic diffusion, advection, and reaction processes at the diffuse interface between solutions. The latter is stretched and folded by the flow heterogeneity, and the concentration field organizes into a lamellae structure, whose elongation dynamics have been shown to play a key role in determining the global reaction kinetics [*Ranz*, 1979; *Ottino*, 1989; *Jiménez and Martel*, 1991]. The effective upscaled reaction rate in these systems is often assumed to be controlled by the interface length and the gradient scale s (the characteristic distance over which the concentration varies), which is generally assumed to grow diffusively with time t, $s \sim \sqrt{Dt}$ where D is the diffusion coefficient. While this approximation may be reasonable for some systems, it disregards the decisive action of compression on the temporal evolution of the gradient size s. Furthermore, it does not describe the temporal dynamics resulting from the merging of the lamellae that form the interface by diffusive coalescence. Here we consider reaction front in porous media, a system for which these two effects are shown to be of critical importance.

©2014. American Geophysical Union. All Rights Reserved.

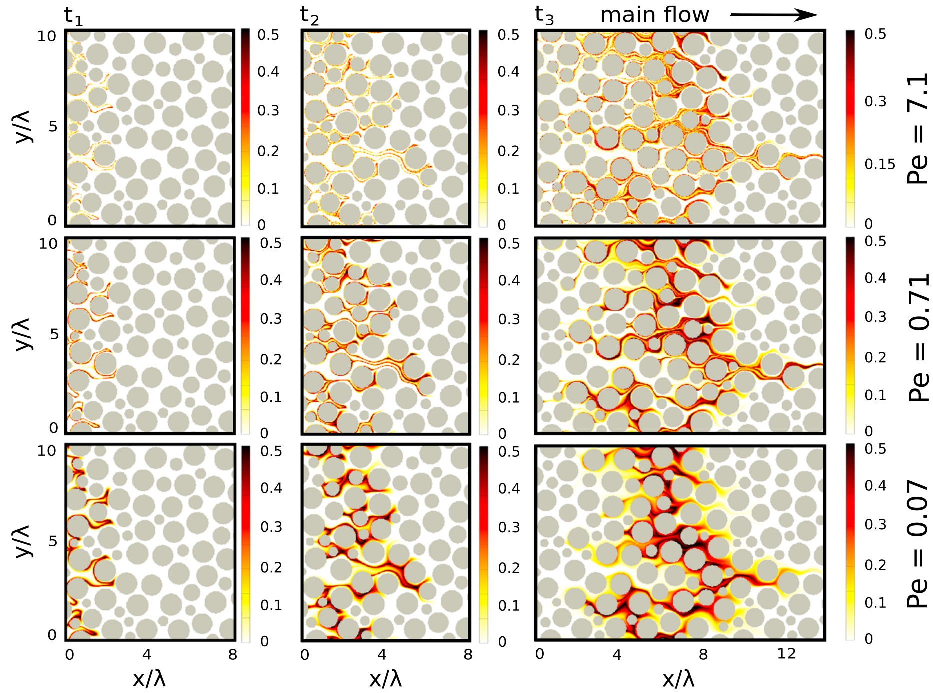

Figure 1. The concentration field of the product C of a fast bimolecular reaction ($A+B \rightarrow C$) at three consecutive times $t_1 = 0.5\tau_a$, $t_2 = 1.6\tau_a$, and $t_3 = 3.5\tau_a$ for three different Pe values (same flow but different diffusion coefficients), where λ represents the average pore size and τ_a is characteristic advection time $\tau_a = \lambda/\bar{v}$ as defined in the text.

We focus on the illustrative case of the irreversible fast bimolecular reaction $A + B \rightarrow C$ in the flow through a porous medium whose heterogeneity determines the front geometry. Here we show that reaction fronts are organized in stretched lamellae, whose deformation and coalescence control the reaction front kinetics. The resulting kinetics differs from that obtained from a purely geometric analysis of the front. We develop a new theoretical approach to explicitly take into account the competition between compression and diffusion in the evolution of concentration gradients, as well as the dynamics of the lamella merging in a unique formulation relating the total mass production to the total diffusive flux of reactants at the front. This novel representation sheds new light on the chemical reaction dynamics in heterogeneous mixing fronts and opens new perspectives for upscaling reaction kinetics in heterogeneous flows.

2. Methods: Pore-Scale Analysis of the Impact of Incomplete Mixing on Reaction Kinetics

To study the impact of mixing processes on the effective reaction kinetics, we consider the two-dimensional heterogeneous polydisperse porous medium shown in Figure 1, characterized by two lengths scales, the average pore size and the average pore throat diameter. The medium is composed of $n_p = 215$ randomly distributed circular grains of different sizes, the average porosity is $\phi = 0.42$, and the average pore size is $\lambda = \sqrt{\phi V/n_p}$, where V is the volume of the porous medium. The typical pore throat size is $h = \lambda/10$. We assume that the reactive flow ($A + B \rightarrow C$) is governed by the combination of the Navier-Stokes (NS) equations and the advection-diffusion-reaction (ADR) equations

$$\frac{\partial c_i(\mathbf{x},t)}{\partial t} = -\nabla \cdot \left[\mathbf{v}(\mathbf{x})c_i(\mathbf{x},t) - D\nabla c_i(\mathbf{x},t)\right] + r_i(\mathbf{x},t), \quad (1)$$

where c_i is the concentration of species i ($i = A, B, C$) and D is the diffusion coefficient, which is assumed to be constant in time and the same for all chemicals. The local reaction rate r_i is given by the law of mass action and set to $r_i = -kc_Ac_B$ for $i = A, B$ and $r_C = kc_Ac_B$.

Initially, the porous medium is fully saturated with a solution containing the chemical species B with concentration $c_B(x, y, t = 0) = c_0$. Through the left boundary a solution containing the dissolved chemical A at concentration $c_A(x = 0, y, t) = c_0$ is injected uniformly for $t > 0$. While mixed, the two reactants undergo

©2014. American Geophysical Union. All Rights Reserved.

the fast bimolecular irreversible reaction $A + B \rightarrow C$. The concentration field of the product C is shown in Figure 1 at three different times for 3 Péclet numbers, as defined and discussed below. The pore-scale fluid velocity field is stationary, the Reynolds number is $Re = 5$, and the mean flow is in the positive x direction. The fluid motion is subject to periodic boundary conditions for velocity at the external boundaries in the x and y directions and no-slip boundary conditions at the grain walls. Pressure is imposed at the external boundaries x direction and periodic the external boundaries y direction.

2.1. Numerical Method

Here we use the Smoothed Particle Hydrodynamics (SPH) method to solve the governing NS and ADR equations. SPH is a Lagrangian method in which fluid is discretized by fluid particles. The details of the SPH method for NS and ADR equations including spatial discretization, time integration, and implementation of the boundary conditions describing reactive flow in porous media can be found in *Tartakovsky et al.* [2007]. The size of the domain is $24\lambda \times 6\lambda$, where λ is the average pore length. It has been divided in 1024×256 pixels. Each pixel is initially filled with 16 particles whose linear size is 0.25 pixels; thus, the total number of particles is $1024 \times 256 \times 16$. The number of fluid particles is $1024 \times 256 \times 16 \times \phi$, where $\phi = 0.42$ is the medium porosity. To implement the no-slip boundary conditions, the solid particles (representing sediment grains) within a distance h from the fluid-solid interface are included in the viscous force term of the SPH momentum conservation (Navier-Stokes) equation. The implementation of the periodic boundary conditions in which fluid particles exit the computational domain and return to the opposite boundary with the same velocities is discussed in detail by *Zhu et al.* [1999].

2.2. Flow and Mixing

The SPH solution of the Navier-Stokes equation for the divergence-free velocity field $\mathbf{v}(\mathbf{x})$ shows existence of a braided network of channels of high velocity as well as stagnation zones with low velocities [*de Anna et al.*, 2013].

The considered reactive flow is characterized by dimensionless Péclet and Damköhler numbers. The Péclet number, defined as $Pe = (h/2)^2\overline{v}/(2D\lambda)$ ($\overline{v}$ is the average flow velocity), is the ratio of the characteristic diffusion time in a pore throat $\tau_D = (h/2)^2/(2D)$ to the advection time in a pore $\tau_a = \lambda/\overline{v}$. The Damköhler number is defined as $Da = \tau_a/\tau_r$, where $\tau_r = 1/(c_0 k)$ is the reaction time. We performed four simulations for $Pe = 0.071$, 0.71, 2.4, and 7.1, which are relevant for low Reynolds number flows through the pore structure (typical of many hydrogeological systems), in which transport is neither diffusion or advection dominated. The Damköhler number is set to $Da = 500$ for all cases. For the observation times under consideration, the reaction can be approximated as instantaneous and therefore mixing limited [*Sanchez-Vila et al.*, 2007]. Three snapshots of product concentration field of C in the porous medium for different Péclet numbers are shown in Figure 1. At early times the interface between the invading and resident fluids, where the reaction product is localized, is stretched due to the flow heterogeneity and develops a lamella-like topology [*Ottino*, 1989; *Kleinfelter et al.*, 2005; *Duplat and Villermaux*, 2008]. For decreasing the Péclet number lamellae tend to merge, which reduces the heterogeneity of the concentration distribution and changes the topology of the mixing zone [*Villermaux and Duplat*, 2003; *Duplat and Villermaux*, 2008; *Le Borgne et al.*, 2013]. This is illustrated in Figure 1, which shows snapshots of the reaction front for three different Péclet numbers. In the following we study the impact of the interface organization on the upscaled reaction kinetics, as quantified by the temporal evolution of the total mass of C,

$$M_C(t) = \int_V c_C(\mathbf{x}, t)\mathrm{d}\mathbf{x}. \tag{2}$$

2.3. Well-Mixed Approximation

In the classical Fickian approach the support volume is assumed to be well mixed and, thus, the evolution of (volume-) averaged concentrations $\overline{c}_i$ can be described by the one-dimensional advection-dispersion-reaction equation [*Whitaker*, 1999]

$$\phi\frac{\partial\overline{c}_i(x,t)}{\partial t} + q\frac{\partial\overline{c}_i(x,t)}{\partial x} - \phi D^*\frac{\partial^2\overline{c}_i(x,t)}{\partial x^2} = r_i^*(x,t), \tag{3}$$

where $i = A, B, C$, ϕ is the porosity and D^* is the sum of the diffusion and the hydrodynamic dispersion coefficients [*Bear*, 1972; *Whitaker*, 1999]. The constant flow velocity q satisfies the Darcy equation [*Bear*, 1972]. In this framework, the reaction rates are given by $r_i^* = -k\overline{c}_A\overline{c}_B$ for $i = A, B$ and $r_C^* = k\overline{c}_A\overline{c}_B$. For the initial and

©2014. American Geophysical Union. All Rights Reserved.

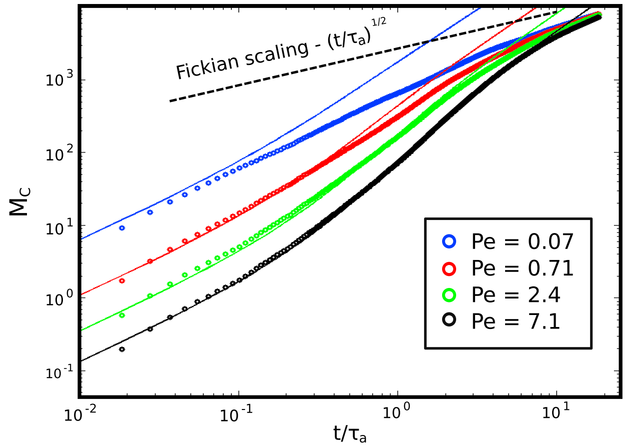

Figure 2. Temporal evolution of the total mass M_C for different Péclet numbers. Time has been rescaled with respect to the characteristic advection time τ_a over a pore length. The obtained temporal scalings differ from the Fickian scaling $t^{1/2}$ (represented by the dashed line). Symbols represent pore-scale numerical simulations, and solid lines represent the analytical model for the stretching regime, equation (9), as defined in the body of the manuscript.

boundary conditions described above and for quasi-instantaneous reaction, one obtains from (3) for the total mass of C [*Gramling et al.*, 2002]

$$M_C(t) = c_0 l_0 \phi \sqrt{\frac{4D^* t}{\pi}}, \quad (4)$$

where l_0 is the domain width.

2.4. Incomplete Mixing

As illustrated in Figure 1, the concentration fields within the pores are not fully mixed. The simulated time evolution of $M_C(t)$ is shown in Figure 2 for different Péclet numbers. It is computed by integrating the concentration of C over all the SPH fluid particles. At all times the total mass of C grows faster than the classical Fickian $\sqrt{t}$ scaling (4) even though its value is smaller since (4) uses the hydrodynamic dispersion coefficient. Furthermore, at late times, the scaling of the total mass is found to be independent of *Pe*, which may appear counterintuitive as reactions are locally directly dependent on diffusion. Theoretical and experimental investigations [*Kitanidis*, 1994; *Kapoor et al.*, 1998; *Gramling et al.*, 2002; *Battiato et al.*, 2009] have shown that the advection-dispersion-reaction equation (3) is insufficient for the correct quantification of Darcy-scale mixing-limited chemical reactions.

Since the reaction is fast, the production of C is limited by the flux of A, or alternatively B, over the interface between the two solutions [*Ottino*, 1989; *Neufeld and Hernandez-Garcia*, 2010], which can be expressed by

$$\frac{\mathrm{d}M_C(t)}{\mathrm{d}t} = D \int_{\Xi(t)} |\nabla c_A(\mathbf{x},t)| \mathrm{d}\Sigma \equiv D\Sigma(t)\overline{|\nabla c_A(\mathbf{x},t)|}, \quad (5)$$

where $\Sigma(t)$ is the length of the interface $\Xi(t)$. The average concentration gradient along the interface $\Xi(t)$, defined by the second equality in (5), can be estimated by $\overline{|\nabla c_A(\mathbf{x},t)|} = c_0/s(t)$ with $s(t)$ the average interface width, which is small compared to the characteristic spreading length of the front. Note that $s(t) \propto \sqrt{Dt}$ for a homogeneous medium which gives the known scaling of $M(t)$ as $M(t) \propto \sqrt{Dt}$; see also (4). In the context of chemical reactions in heterogeneous flows, current models for the global reaction kinetics do not account for the competition between lamellae compression and diffusion in the dynamics of the reactive front width $s(t)$, which in some cases is assumed to be constant [*Ottino*, 1989] and in others to grow diffusively as $\sqrt{Dt}$ [*Neufeld and Hernandez-Garcia*, 2010; *Jiménez and Martel*, 1991].

3. Results and Discussion: Temporal Regimes of Effective Reaction Kinetics

3.1. Stretching Regime

At early times the interface between reactants is organized in complex elongated structures which form a lamella-like topology. Lamellae can be seen as a decomposition of the front line into elementary segments [*Meunier and Villermaux*, 2003], which are stretched by the local flow field and, since diffusion has not had sufficient time to merge them, they can be considered independent (see Figure 3). In this regime, the interface width $s(t)$ evolves through the competition of molecular diffusion, which tends to increase it, and compression perpendicular to the local stretching direction. The average compression rate can be estimated as the negative of the interface elongation rate $\frac{1}{\Sigma(t)}\frac{\mathrm{d}\Sigma(t)}{\mathrm{d}t}$ [*Le Borgne et al.*, 2011; *Villermaux*, 2012; *Le Borgne et al.*, 2013]. Due to the assumed incompressibility, the flow conserve fluid volumes; thus, the balance equation for the average front width is

$$\frac{1}{s(t)}\frac{\mathrm{d}s(t)}{\mathrm{d}t} = \frac{D}{s(t)^2} - \frac{1}{\Sigma(t)}\frac{\mathrm{d}\Sigma(t)}{\mathrm{d}t}. \quad (6)$$

©2014. American Geophysical Union. All Rights Reserved.

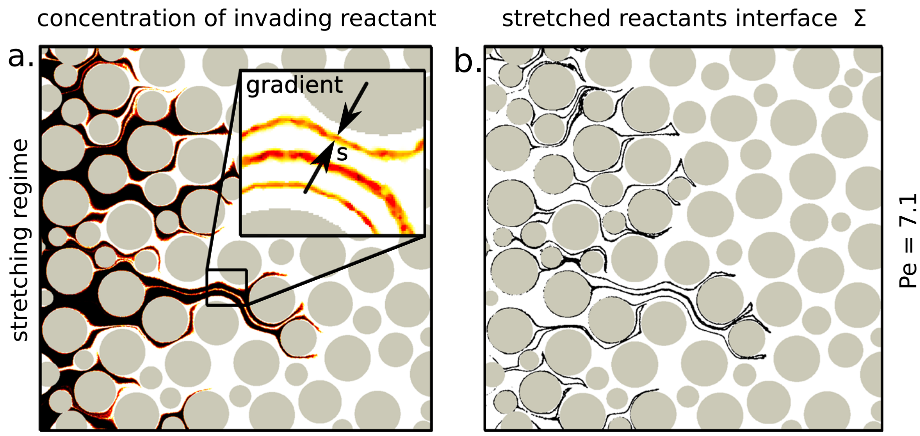

Figure 3. (a) The concentration field of the invading reactant A at time $t = 4.2\tau_a$ and $Pe = 7.1$. At this time the system is in the stretching regime, and the reaction front is organized in independent stretched lamellae. The inset displays a zoom of the reactant gradient and its width $s(t)$. (b) The reactants interface Ξ, defined as the portion of the system where $\nabla c_A(\mathbf{x}, t) > 0$.

The dynamics of the interface length $\Sigma(t)$ are determined by the flow kinematics. A detailed discussion about the origin of different temporal behaviors of $\Sigma(t)$ for different type of stochastic stretching processes is provided in *Duplat et al.* [2010] and for heterogeneous Darcy flows in *Le Borgne et al.* [2013]. For the porous medium considered here, we defined the interface between reactants Ξ as the portion of the system where $\nabla c_A(\mathbf{x}, t) > 0$ (see Figure 3) and its length Σ as the sum over the set of points composing the line where $c_A = c_0/2$. The numerical estimation of the length of the interface is shown in Figure 4 for different Péclet numbers. At early times $\Sigma(t)$ is found to evolve linearly as

$$\Sigma(t) = l_0\sqrt{\phi}(1 + \gamma t), \tag{7}$$

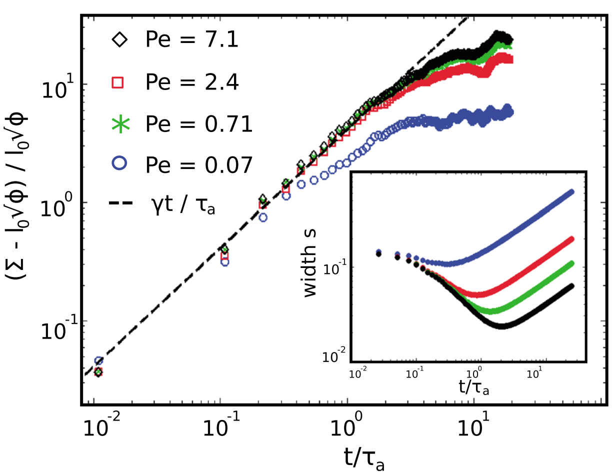

Figure 4. The main figure displays the temporal evolution of the reactants interface length Σ that has been measured for the four different Péclet number values (symbols of different color): the linear trend breaks down as the reactant lamellae start to coalesce by diffusion. The inset shows the analytical solution for the reactants interface width s, equation (8) (using the same color for the same Pe): as the lamellae are independent and do not interact, the interface width decreases due to compression induced by the flow stretching. At later times the diffusive coalescence of lamellae leads to the diffusive evolution of $s \propto \sqrt{t}$. Note that the time is rescaled with respect to the characteristic advection time τ_a over a pore length; all the length are expressed in units of the average pore size λ.

where γ is the elongation rate and $l_0\sqrt{\phi}$ is the initial reactants interface length. This observation is consistent with the value of $\gamma \approx 5$ obtained from the pair separation statistics of advected fluid particles originally distributed along the injection line. The same scaling has been observed within a pore-scale experiment by *de Anna et al.* [2014]. Inserting (7) into (6) and solving for $s(t)$, the interface width is [*Villermaux*, 2012]

$$s(t) = s_0\sqrt{\frac{3\beta - 2 + 2(1 + \gamma t)^3}{3\beta(1 + \gamma t)^2}}, \tag{8}$$

where $\beta = s_0^2\gamma/D$ and $s_0 = s(0)$ is the initial width of the reactive front. The temporal evolution of $s(t)$ predicted by this model is shown in the inset of Figure 4. Due to stretching, the lamella width $s(t)$ decreases until the mixing time $\tau_m \propto \beta^{1/3}$ when compression and diffusive growth equilibrate

©2014. American Geophysical Union. All Rights Reserved.

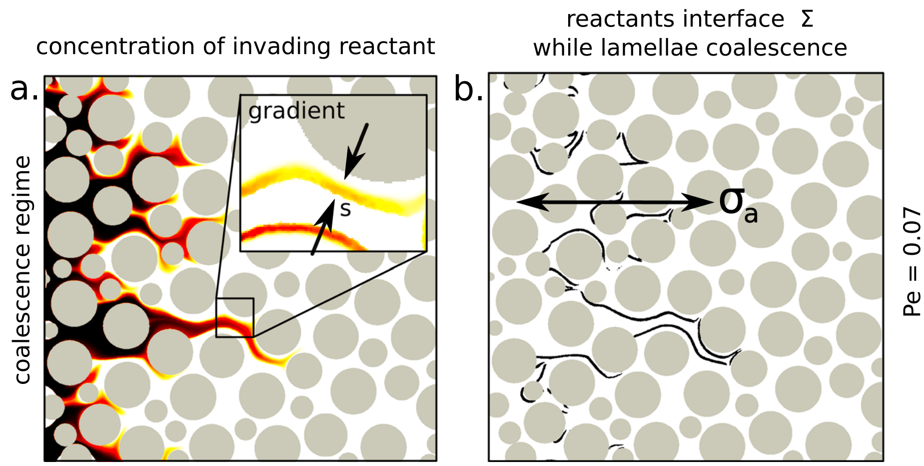

Figure 5. (a) The concentration of the invading reactant A at time $t = 4.2\tau_a$ and $Pe = 0.07$: the reaction front here is made of lamellae bundles which derives from the diffusive coalescence of reactants lamellae. The inset shows the gradient of the invading reactant A and its thickness $s(t)$. (b) The reactants interface $\Xi(t)$. For decreasing Pe the coalescence of adjacent lamellas reduces the number of lamellae aggregates n_b, compared to Figure 3.

[*Villermaux*, 2012]. After this time, the width $s(t)$ grows diffusively as $s(t) \propto \sqrt{Dt}$. Inserting (7) in (5) and subsequently integrating, we obtain

$$M_C(t) = Dc_0 l_0 \sqrt{\phi} \int_0^t \frac{1+\gamma t'}{s(t')} \mathrm{d}t'. \tag{9}$$

The mixing time τ_m marks the transition to the regime in which lamellae start interacting and coalescing due to diffusion. Figure 2 shows excellent agreement between the observed $M_C(t)$ and the prediction of the analytical model (9) for times $t < \tau_m$ with γ and s_0 determined from the pore-scale simulations.

3.2. Coalescence Regime

At times $t > \tau_m$ the different elements of the interface cannot be considered independent as they interact by diffusion. Coalescence changes the front topology through the formation of aggregate lamellae bundles, as illustrated in Figure 5, and this is known to occur in a variety of flow fields [*Villermaux and Duplat*, 2003; *Duplat and Villermaux*, 2008; *Le Borgne et al.*, 2013]. We estimate the evolution of $\Sigma(t)$ in the coalescence regime as the average length $l_b(t)$ of the lamellae bundles times the number of bundles $n_b(t)$ at time t. The average lamella bundle length $l_b(t)$ can be measured by the width of the reaction front. This width on the other hand can be quantified by the longitudinal spreading length $\sigma_a(t)$ of fluid particles, which is defined as

$$\sigma_a^2(t) = \langle [\delta x(t) - \langle \delta x(t) \rangle]^2 \rangle, \tag{10}$$

with $\delta x(t) = x(t) - x(0)$ and $x(t)$ the longitudinal coordinate of the trajectory of a Lagrangian fluid particle (see also Figure 5). The angular brackets represent the average overall fluid particles. As illustrated in Figures 3 and 5, $n_b(t)$ decreases as bundles coalesce to form larger aggregates. The number of bundles in a pore is expected to be inversely proportional to the interface width $s(t)$, which limits the available space for separate bundles to coexist (see Figure 5). As $s(t)$ increases, bundles keep merging and their number decreases accordingly so that $\Sigma(t) = n_b(t) l_b(t) \propto \sigma_a(t)/s(t)$. Notice that, as outlined above, for $t > \tau_m$ $s(t) \propto \sqrt{Dt}$. Thus, we obtain from (5) for the produced mass $M_C(t)$ at times $t > \tau_m$

$$\frac{\mathrm{d}M_C(t)}{\mathrm{d}t} \propto \frac{Dc_0\sigma_a(t)}{s(t)^2} \propto \frac{c_0\sigma_a(t)}{t}, \tag{11}$$

which reflects the lack of sensitivity of $M_C(t)$ to variations in Pe as observed in Figure 2. This phenomenon can be explained by the fact that local diffusive growth contributes to bundle coalescence but not to the growth of the mixing area. The net result is that the dominant effect for mixing in this regime is the advective spreading of fluid volumes. Here $\sigma_a(t)$ scales as a power law of time, see the inset of Figure 2, so that direct integration of (11) gives $M_C(t) \propto \sigma_a(t)$. To provide a global picture of the reaction dynamics, we

©2014. American Geophysical Union. All Rights Reserved.

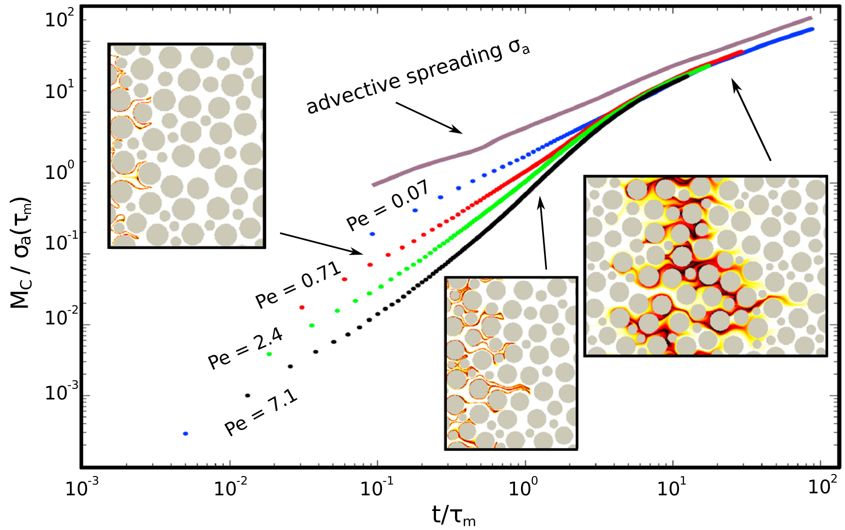

Figure 6. The rescaled mass of produced C, $M_c/\sigma_a(\tau_m)$ versus the rescaled time t/τ_m for different Péclet number values (symbols). The solid line shows the scaling of the advective spreading σ_a.

rescale time with respect to the mixing time τ_m and cumulative mass $M_C(t)$ with respect to $\sigma_a(\tau_m)$ as shown in Figure 6. For times $t \gg \tau_m$ all curves scale as $\sigma_a(t)$ as suggested by (11). The temporal scaling of the advective dispersion length $\sigma_a(t)$ in porous media is persistently non-Fickian [*de Anna et al.*, 2013]. Here the origin of the non-Fickian scaling of σ_a^2 is due to strong intermittent properties of flow velocities as reflected by their non-Gaussian distribution and their long-range temporal correlation along streamlines [*Le Borgne et al.*, 2008]. This implies that the effective reaction kinetics is expected to differ from the well-mixed Fickian behavior of equation (4) over a large range of temporal scales.

4. Conclusions

This paper shows the development of filamentary or lamellar structures in mixing-limited reactive fronts flowing through porous media. The dynamics of these lamella-like structures, which evolve through compression, diffusion, and merging, is shown to govern the temporal evolution of the global reaction rates. The proposed predictive model relates the global kinetics to the flow kinematics (stretching rate γ and advective spreading size dynamics $\sigma_a(t)$) for the two identified regimes of stretching and coalescence of the lamellae structures. Hence, the issue of predicting upscaled reaction kinetics reduces to the quantification of purely advective properties (γ, σ_a), whose relation with structural disorder properties is the subject of current investigations. The developed general framework can be extended to $d = 3$ dimensions based on the analysis of the stretching of the interface area between invading and displaced solution and coalescence as the interface aligns with the flow velocity [*Duplat and Villermaux*, 2008]. These findings have direct implications for effective reactive transport modeling in a range of applications, such as convective-mixing processes in carbon dioxide storage, contaminant transport and reactivity in hydrological systems, or mixing-driven biochemical processes in filters and living tissues. Furthermore, since the basic processes involved occur in a wide range of heterogeneous flows, the proposed theoretical framework may serve for understanding and quantifying reaction front kinetics beyond porous media flows.

Acknowledgments
P. de Anna and T. Le Borgne acknowledge the financial support of the European Commission through FP7 ITN project IMVUL (grant agreement 212298) and Marie Curie ERG grant Reactive Flows (grant agreement 230947). M. Dentz acknowledges the support of the FP7 EU project PANACEA (grant 282900) and the Spanish Ministry of Economy and Competitivity through the project HEART (CGL2010- 18450). A. Tartakovsky was supported by the Office of Advance Scientific Computational Research of the U.S. Department of Energy. E. Villermaux is gratefully acknowledged for stimulating discussions.

The Editor thanks Diogo Bolster and an anonymous reviewer for their assistance in evaluating this paper.

References

Battiato, I., D. M. Tartakovsky, A. M. Tartakovsky, and T. Scheibe (2009), On breakdown of macroscopic models of mixing-controlled heterogeneous reactions in porous media, *Adv. Water Resour.*, *32*(11), 1664–1673.

Bear, J. (1972), *Dynamics of Fluids in Porous Media*, American Elsevier, New York.

de Anna, P., T. Le Borgne, M. Dentz, A. Tartakovsky, D. Bolster, and P. Davy (2013), Flow intermittency, dispersion, and correlated continuous time random walks in porous media, *Phys. Rev. Lett.*, *101*, 184,502.

de Anna, P., J. Jimenez-Martinez, H. Tabuteau, R. Turuban, T. Le Borgne, M. Derrien, and Y. Méheust (2014), Mixing and reaction kinetics in porous media: An experimental pore scale quantification, *Environ. Sci. Technol.*, *48*, 508–516.

Dentz, M., T. Le Borgne, A. Englert, and B. Bijeljic (2011), Mixing, spreading and reaction in heterogeneous media: A brief review, *J. Contam. Hydrol.*, *120–121*, 1–17, doi:10.1016/j.jconhyd.2010.05.002.

De Wit, A. (2001), Fingering of chemical fronts in porous media, *Phys. Rev. Lett.*, *87*, 054,502.

Duplat, J., and E. Villermaux (2008), Mixing by random stirring in confined mixtures, *J. Fluid Mech.*, *617*, 51–86.

 ©2014. American Geophysical Union. All Rights Reserved.

Duplat, J., C. Innocenti, and E. Villermaux (2010), A non-sequential turbulent mixing process, *Phys. Fluids*, *22*, 035,104.

Durham, W., E. Climent, and R. Stocker (2011), Gyrotaxis in a steady vortical flow, *Phys. Rev. Lett.*, *106*, 238,102.

Ennis-King, J., and L. Paterson (2005), Role of convective mixing in the long-term storage of carbon dioxide in deep saline formations, *Soc. Petrol. Eng. J.*, *10*, 349–356.

Gramling, C. M., C. F. Harvey, and L. C. Meigs (2002), Reactive transport in porous media: A comparison of model prediction with laboratory visualization, *Environ. Sci. Technol.*, *36*(11), 2508–2514.

Jamtveit, B., A. Malthe-Sorenssen, and O. Kostenko (2008), Reaction enhanced permeability during retrogressive metamorphism, *Earth Planet. Sci. Lett.*, *267*, 620–627.

Jiménez, J., and C. Martel (1991), Fractal interfaces and product generation in the two-dimensional mixing layer, *Phys. Fluids A*, *3*, 1261–1268.

Kapoor, V., C. Jafvert, and D. Lyn (1998), Experimental study of a bimolecular reaction in Poiseuille flows, *Water Resour. Res.*, *34*, 1997–2004.

Kirchner, J., and C. Neal (2013), Universal fractal scaling in stream chemistry and its implications for solute transport and water quality trend detection, *Proc. Natl. Acad. Sci.*, *110*, 12,213–12,218.

Kitanidis, P. K. (1994), The concept of the dilution index, *Water Resour. Res.*, *30*(7), 2011–2026.

Kleinfelter, N., M. Moroni, and J. H. Cushman (2005), Application of the finite-size Lyapunov exponent to particle tracking velocimetry in fluid mechanics experiments, *Phys. Rev. E*, *72*, 056,306.

Le Borgne, T., M. Dentz, and J. Carrera (2008), Lagrangian statistical model for transport in highly heterogeneous velocity fields, *Phys. Rev. Lett.*, *101*, 090,601.

Le Borgne, T., M. Dentz, P. Davy, D. Bolster, J. Carrera, J. de Dreuzy, and O. Bour (2011), Persistence of incomplete mixing: A key to anomalous transport, *Phys. Rev. E*, *84*, 015,301.

Le Borgne, T., M. Dentz, and E. Villermaux (2013), Stretching, coalescence and mixing in porous media, *Phys. Rev. Lett.*, *110*, 204,501.

Malthe-Sorenssen, A., B. Jamtveit, and P. Meakin (2006), Fracture patterns generated by diffusion controlled volume changing reactions, *Phys. Rev. Lett.*, *96*, 245,501.

Meunier, P., and E. Villermaux (2003), How vortices mix, *J. Fluid Mech.*, *476*(213-22).

Neufeld, Z., and E. Hernandez-Garcia (2010), *Chemical and Biological Processes in Fluid Flows: A Dynamical System Approach*, Imperial College Press, London, U. K.

Ottino, J. (1989), *The Kinematics of Mixing: Stretching, Chaos, and Transport*, Cambridge Univ. Press, Cambridge, U. K.

Polizzotto, M. L., C. F. Harvey, S. R. Sutton, and S. Fendorf (2005), Processes conducive to the release and transport of arsenic into aquifers of Bangladesh, *Proc. Natl. Acad. Sci.*, *102*, 18,819–18,823.

Ranz, E. W. (1979), Applications of a stretch model for mixing, diffusion, and reaction in laminar and turbulent flows, *AIChE J.*, *25*(1), 41–47.

Renard, F., J. Gratier, P. Ortoleva, E. Brosse, and B. Bazin (1998), Self-organization during reactive fluid flow in a porous medium, *Geophys. Res. Lett.*, *25*, 385–388.

Sanchez-Vila, X., M. Dentz, and L. Donado (2007), Transport-controlled reaction rates under local non-equilibrium conditions, *Geophys. Res. Lett.*, *34*, L10404, doi:10.1029/2007GL029410.

Sebilo, M., B. Mayer, B. Nicolardot, G. Pinay, and A. Mariotti (2013), Long-term fate of nitrate fertilizer in agricultural soils, *Proc. Natl. Acad. Sci.*, *110*, 18,185–18,189, doi:10.1073/pnas.1305372110.

Szulczewski, M. L., C. W. MacMinn, H. J. Herzog, and R. Juanes (2012), Lifetime of carbon capture and storage as a climate-change mitigation technology, *Proc. Natl. Acad. Sci*, *109*, 5185–5189.

Tartakovsky, A. M., P. Meakin, T. D. Scheibe, and B. D. Wood (2007), A smoothed particle hydrodynamics model for reactive transport and mineral precipitation in porous and fractured porous media, *Water Resour. Res.*, *43*(5), W05437, doi:10.1029/2005WR004770.

Tartakovsky, A. M., G. D. Tartakovsky, and T. D. Scheibe (2009), Effects of incomplete mixing on multicomponent reactive transport, *Adv. Water Resour.*, *32*(11), 1674–1679.

Villermaux, E. (2012), Mixing by porous media, *C.R. Mec.*, *340*, 933–943.

Villermaux, E., and J. Duplat (2003), Mixing as an aggregation process, *Phys. Rev. Lett.*, *91*, 184,501.

Whitaker, S. (1999), *The Method of Volume Averaging*, vol. 1, Springer, Houten, Netherlands.

Zhu, Y., P. Fox, and J. Morris (1999), A pore-scale numerical model for flow through porous media, *Int. J. Numer. Anal. Methods Geomech.*, *23*, 881–904.

 ©2014. American Geophysical Union. All Rights Reserved.